

# 193nm imaging using a small-field high-resolution resist exposure tool

Nadeem H. Rizvi, Malcolm C. Gower, Dominic Ashworth, Neil Sykes, Phil T. Rumsby  
Bruce W. Smith\*, Francis N. Goodall and Ron A. Lawes

Exitech Limited, Hanborough Park, Long Hanborough, Oxford OX8 8LH, England  
Microelectronic Engineering Department, Rochester Institute of Technology, Rochester, NY 14623-5604  
Central Microstructure Laboratory, Rutherford Appleton Laboratory, Chilton, OXI 1 0QX, England

## ABSTRACT

A 193nm excimer laser microstepper has been developed for deep UV photolithography research at this wavelength. The system incorporates a x10, 0.5NA, 4mm field diameter, high-resolution imaging lens of either all-refractive or catadioptric design. An all-fused silica refractive lens has been used in the results reported here to carry out exposures in polymethylmethacrylate and polyvinylphenol photoresists. Well-resolved images of 0.2 $\mu$ m dense lines and spaces and 0.35 $\mu$ m diameter contact holes have been produced in PMMA and polyvinylphenol resists.

**Keywords:** 193nm lithography, silylation, top-surface imaging, photoresists, excimer lasers, line-narrowing.

## 1. INTRODUCTION

Much interest has recently been focussed on extending existing deep UV photolithography technology to produce sub-0.2 $\mu$ m features for future generations of >1Gbit DRAM semiconductor memory devices. Deep UV photolithography with an ArF excimer laser source at a wavelength of 193nm has been identified as a very attractive candidate for a potential process and as a tool capable of achieving these design rules<sup>1,2</sup>. The emerging manufacturing implementation of 248nm lithography stepper tools serve as a guide for some of the problems that arise in the use excimer laser exposure systems but many challenges need to be overcome before photolithography at 193nm can be seriously considered as a manufacturing process.

As is well known, the depth of focus (DOF) of optical projection systems is proportional to  $\lambda/NA^2$ , where  $\lambda$  is the optical wavelength and NA is the numerical aperture of the imaging lens. For 0.2 $\mu$ m resolution at 193nm, the DOF falls to <1 $\mu$ m and so image enhancement techniques such as the use of phase-shift masks<sup>3</sup> or top-surface imaging (TSI)<sup>4</sup> need to be investigated. Other crucial areas also needing to be assessed and developed at 193nm include high quality fused silica and CaF<sub>2</sub> optical materials, high-NA lenses, lifetime testing of optical components, illumination issues such as beam homogenisation, off axis imaging and development of suitable photoresists.

In this paper we report results using an Exitech Series 8000 ArF excimer laser microstepper designed for carrying out deep UV photolithography R&D at 193nm. TSI and single-layer imaging work is presented which demonstrates resolutions of <0.2 $\mu$ m. Some of the issues mentioned above are also addressed.

## 2. EXPERIMENTAL

### 2.1 MICROSTEPPER SYSTEM

#### 2.1.1 ArF Laser Source

The Exitech Series 8000 193nm microstepper, shown in Figure 1 and depicted schematically in Figure 2, incorporates a Lambda Physik LPX210i ArF excimer laser as the deep-UV source. When operated at 193nm, this laser produces 32W of average power at its maximum repetition rate of 100Hz within the full 370pm FWHM bandwidth of the ArF transition.



Figure 1. Exitech 193nm excimer laser microstepper system

When modified using a specially developed line-narrowing module, the laser produces an average output power of 3 W in a minimum linewidth of <math><5\text{pm}</math> FWHM. With this module, the laser may be tuned between wavelengths of 192.75 - 193.75nm and the bandwidth selected between 370-5pm FWHM.

### 2.1.2 Illumination optics

The beam from the laser is shaped to be 28mm x 28mm at the reticle plane. A double fly's eye homogeniser arrangement produces a reticle illumination uniformity of  $< \pm 5\%$  RMS/pulse. The degree of beam shaping and homogenisation depend on the type of lens objective being used. A CNC-controlled variable attenuator in the beam line is used to set the single pulse exposure dose on the wafer. For carrying out exposures with either s- or p-polarized 193nm radiation, a removable polarizer can be inserted into the beam train. All mirrors are coated with high damage threshold dielectric coatings while lenses and other transmissive optics are AR-coated to minimise Fresnel reflection losses. To reduce the absorption by atmospheric oxygen and to prevent the formation of ozone and contamination of the optical train, the entire system from the laser to the condenser lens is purged with dry nitrogen gas. Variable and fixed apertures incorporated in the beam homogeniser unit are used to adjust the partial coherence factor and provide off axis illumination configurations.

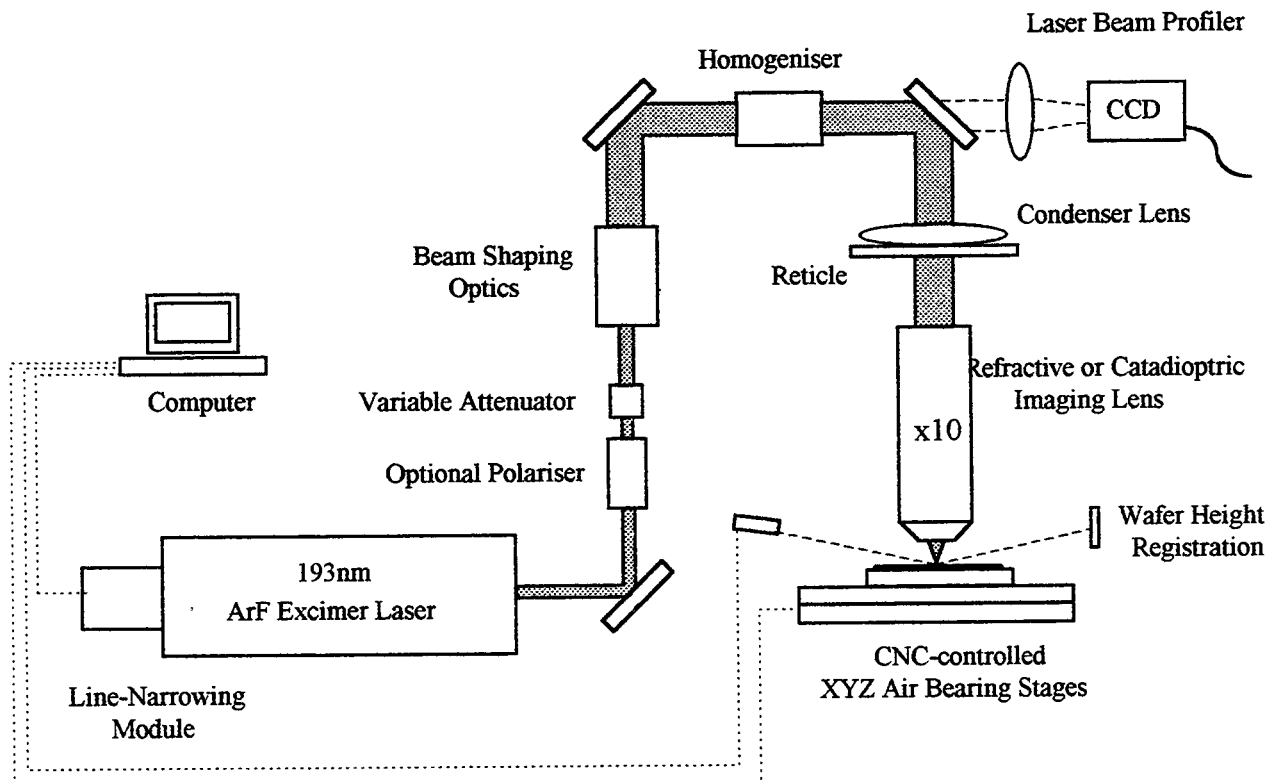


Figure 2. Schematic diagram of 193nm excimer laser lithography exposure

The reticle, imaging lens and wafer stages are all mounted on a common granite block structure to provide precise mechanical stability. To allow comparative studies to be made between exposure work at 193nm and 248nm, the entire microstepper can be readily converted for use at either wavelength.

### 2.1.3 Imaging optics

The tool is designed to be used with either all-refractive or reflective catadioptric 0.5NA, x10 193nm imaging lens objectives having image field diameters of 4mm. The lenses were designed using CODE V<sup>®</sup> and tested interferometrically during fabrication. Chromatic aberration of the ten element all-refractive fused silica lens, shown in Figure 3, was eliminated by reducing the bandwidth of the ArF laser to 5pm FWHM. All surfaces were coated with spun-on colloidal silica antireflection coatings and the mirrors of the catadioptric lens were coated with multilayer dielectric coatings having a reflectivity of >95% at 193nm. For this lens, seven fused silica corrective elements were used.

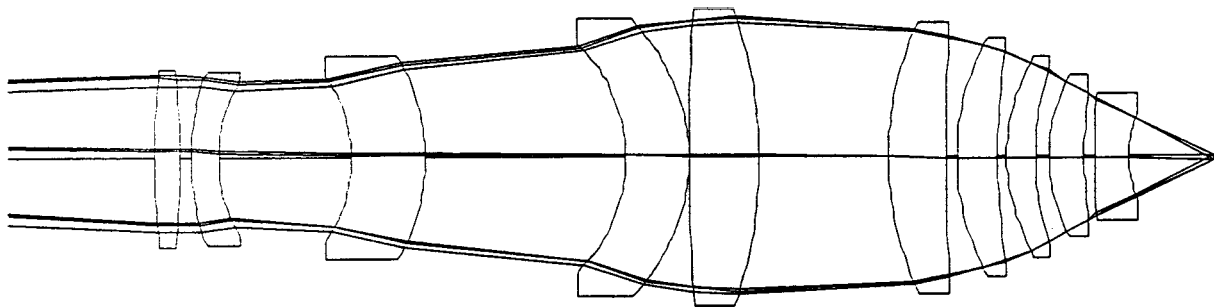


Figure 3. Design of x10, 0.5NA all-refractive fused silica lens

### 2.1.4 Wafer positioning and registration

Precision CNC-controlled air-bearing stages mounted on a granite base are used to provide both short and long-term lateral stability of the wafer during an exposure. Using capacitive nanosensors, measurements from milliseconds to several minutes have shown that the wafer remains stationary to within  $< \pm 10\text{nm}$ .

Either 6" or 8" wafers can be used with this microstepper system and these are held on a precision vacuum chuck. A CNC-controlled position-sensitive detection (PSD) system is used for focal registration and to provide an autofocus method for automated focal-dose exposure scans. Focal position and wafer surface height are registered and controlled to less than 100nm.

Coarse determination of the focal plane of the lens is made with an accuracy of  $\sim 10\mu\text{m}$  using a microscope objective and CCD camera integrated in the wafer chuck. This allows a fluorescent image of the reticle, induced by the 193nm radiation in borosilicate glass wafers, to be brought into focus and the surface of the glass wafer registered with the PSD system.

### 2.1.5 Beam diagnostics

A CCD camera based Exitech P256NG 193nm laser beam profiling system is incorporated in the microstepper for monitoring the illumination profile at the reticle plane in real time during an exposure and for calibrating measurements of pulse energy variation and exposure dose.

In a beam diagnostics section of the tool (Series 7000) shown in the centre of the picture in Figure 1, a high-resolution Exitech Minispec laser spectrometer (~1pm resolution at 193 and 248nm) incorporated in the beam line provides real-time monitoring of the laser wavelength, linewidth and stability. When line-narrowed, the centre wavelength of the laser output is maintained to within  $\pm 2$ pm by a computer-controlled active feedback system developed by Exitech. This ensures stability and reproducibility of the laser spectral output during exposures and nullifies any thermally- or mechanically-induced variations in the laser wavelength. The temporal characteristics and energy of the laser pulses are measured using a silicon PIN photodiode and a joulemeter respectively.

To determine the refractive index and absorptive properties of developmental photoresists, the Series 7000 section of the tool can also be used to measure the reflectance of photoresists or thin films at 193nm (or other excimer laser UV wavelengths) as a function of angle of incidence under a computer-controlled environment.

### 2.1.6 System control

Functions such as the laser parameters, exposure dose setting, wafer-positioning and focussing are CNC-controlled from a single console operating under a PC Windows<sup>®</sup> platform enabling fully automatic exposures to be performed. The autofocus system checks and adjusts the focal position of the resist before each site on a wafer is exposed and conditions such as dose, focal position, site identification, etc. for each site are stored in the system computer. A wafer map is produced after each exposure detailing the exact parameters of the exposed sites. After each exposure run, illumination beam profiles and the spectral characteristics of the laser can also be archived.

## **2.2 PHOTORESISTS**

Currently there are very few photoresist candidates suitable for carrying out deep UV exposure work at 193nm. In the work reported here, we have concentrated on using two photopolymers - polymethylmethacrylate (PMMA) and polyvinylphenol (MX-P8).

The PMMA resist (Shipley 950PMMA C9) was spun to a thickness of 0.22 $\mu$ m onto a 0.3 $\mu$ m-thick layer of novolac (Shipley Microposit 2415) which acted as an anti-reflection layer between the substrate and the resist. Chlorobenzene was used as the solvent for the PMMA in a 1:1 mixture and baked for 1min at 120°C prior to exposure. Post-exposure development was carried out in a 1:1 mixture (by volume) of isopropyl alcohol (IPA) and methylisobutyl ketone (M BK) for 1 min followed by a standing rinse in IPA for 15sec.

For top-surface imaging studies at 193nm, the MX-P8 resist (Microlithography Chemical Corp.) was spun to give a thickness of 0.3 $\mu$ m. The same pre-exposure bake conditions were used as for PMMA. After exposure the resist was silylated in the vapour phase by injecting dimethylsilyldimethylamine (DMSDMA, Microlithography Chemical Corp.) at 15mbar pressure into a temperature-controlled oven at 120°C for 1min. Reactive-ion etching was then performed using an Oxford Plasma Technology parallel-plate RIE80 system with O<sub>2</sub> gas (60W, 50sccm, 8min). No skin etch was performed.

### **3. RESULTS**

Results presented here were obtained using the all-refractive, 0.5NA, fused silica x10 imaging lens depicted in Figure 3. The laser was operated at a linewidth of 5pm with a typical fluence on the wafer of  $\sim 300\mu\text{J}/\text{cm}^2$  per pulse. Since the sensitivity at 193nm of PMMA resist is  $\sim 1\text{J}/\text{cm}^2$ , operation at a laser repetition rate of 100Hz and these fluences give an exposure duration of around a minute. In contrast, the exposure dose for MX-P8 resist is only several tens of  $\text{mJ}/\text{cm}^2$  so only a few seconds are required to expose each site. Exact exposure doses are set by CNC-controlling the integrated dose to the nearest integer number of laser pulses.

SEM images of well-resolved  $0.2\mu\text{m}$  lines and spaces imaged into PMMA photoresist are shown in Figure 4. The  $0.2\mu\text{m}$  features were produced uniformly and reproducibly across the field for doses in the range of  $1.1\text{--}1.3\text{ J}/\text{cm}^2$  and the partial coherence factor was 0.55 for these exposures. We attribute the slight bubbling of the unexposed surface regions to the wet development process.

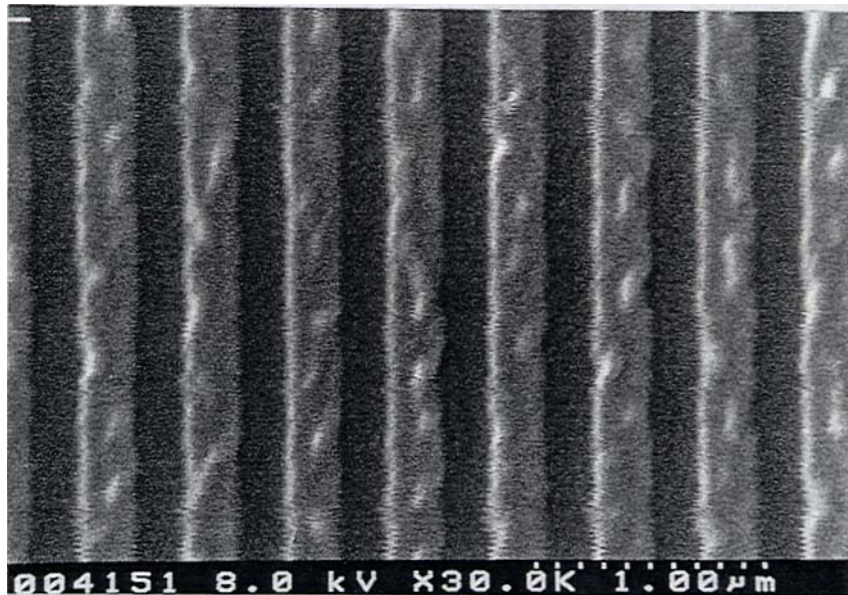


Figure 4.  $0.2\mu\text{m}$  lines and spaces in PMMA

Figures 5 and 6 shows  $0.2\mu\text{m}$  lines and spaces produced in MX-P8 using TSI. The modulations observed in the side-walls of the lines are due to the plasma etch process and are not optically-induced.

Contact holes were also imaged in MX-P8 resist. The partial coherence factor for the contact hole exposures was set to be 0.4 and focal dose scans were again conducted to determine the optimum conditions. The preliminary results of  $0.4\mu\text{m}$  and  $0.35\mu\text{m}$  holes are shown in Figure 7.  $0.3\mu\text{m}$  contact holes have also been imaged but with lesser clarity. Further work is already underway to optimise the sub- $0.3\mu\text{m}$  imaging of contact holes structures.

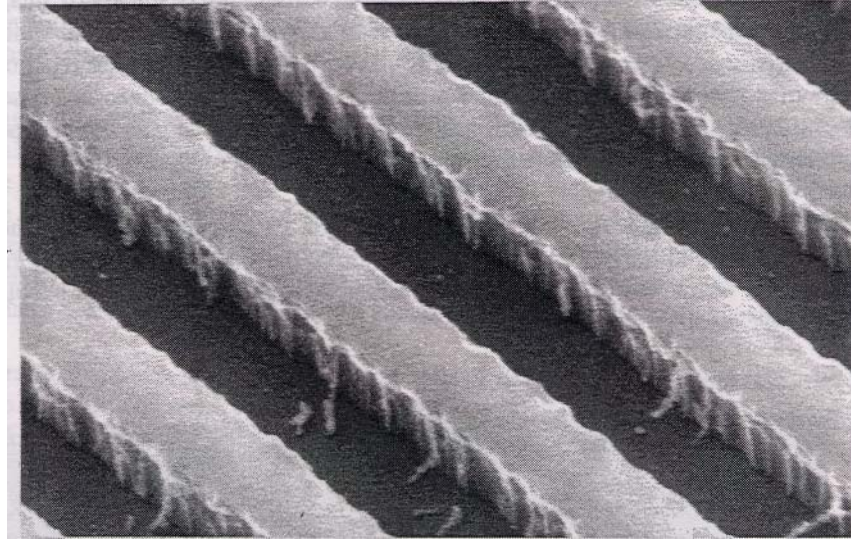


Figure 5. 0.2µm lines and spaces in MX-P8 imaged using top-surface imaging

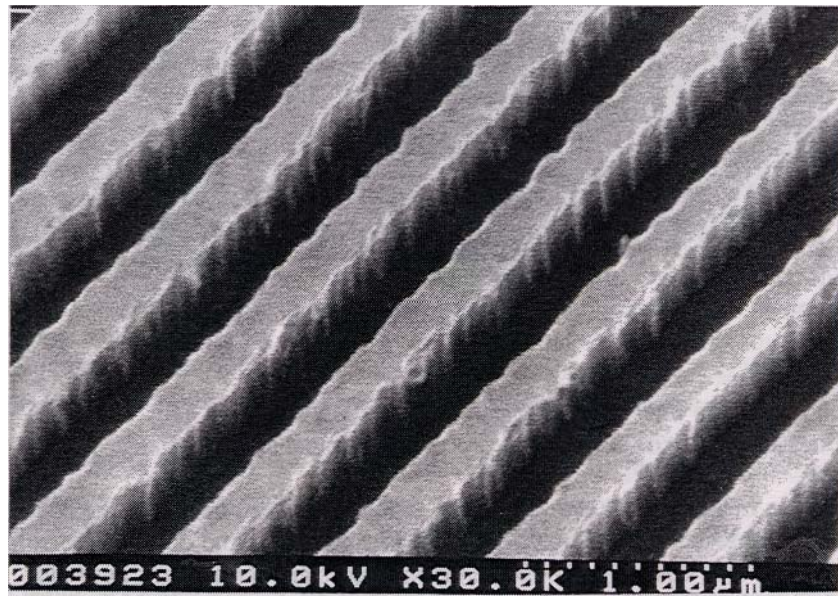


Figure 6. 0.2µm lines and spaces in MX-P8 imaged using top-surface imaging

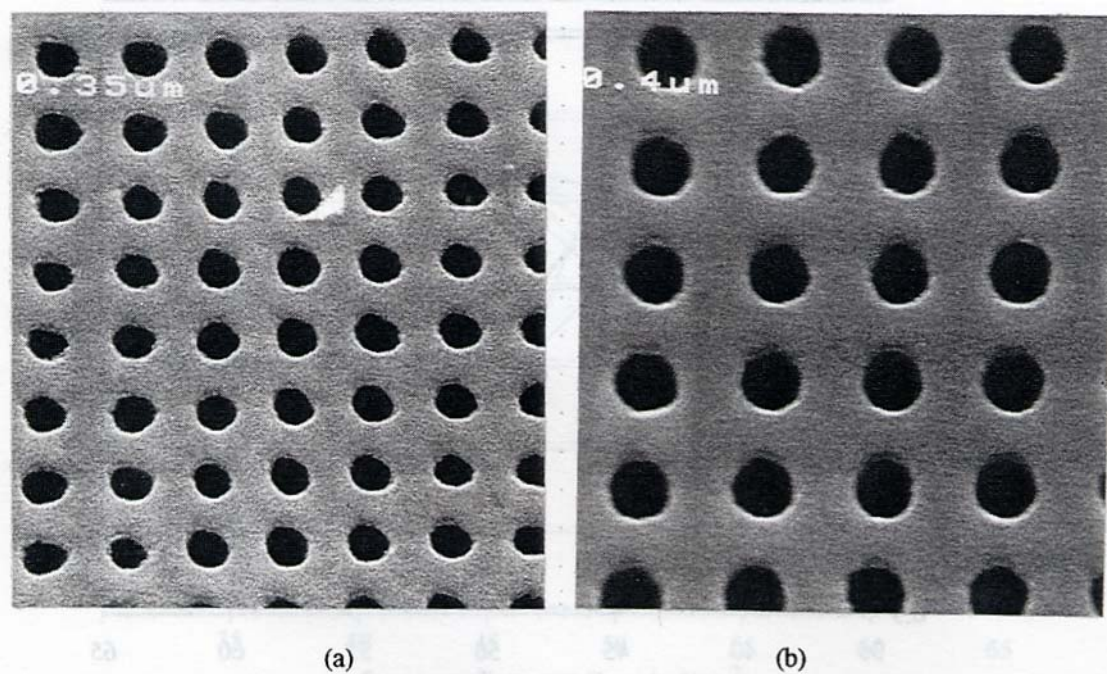


Figure 7. (a) 0.3 $\mu$ m and (b) 0.4 $\mu$ m contact holes imaged in MX-P8 resist using top-surface imaging

Measurements of the process latitude in MX-P8 for lines and spaces ranging from 0.2 $\mu$ m to 0.35 $\mu$ m are shown in Figures 8 and 9. The exposure dose is plotted against the ratio of the width of the lines to the line/space period for different focal positions. These plots relate to the initial characterisation of the microstepper and were intended to give a broad indication of the overall performance of the exposure system and TSI photoresist. It can be seen that the dose was found to be more critical than the focal position. This highlights one of the benefits of TSI in that this process is far more tolerant to defocussing since only a small portion of the top layer of the resist needs to be within the depth of focus of the lens for the image to be transferred well into the bulk of the resist<sup>5</sup>. The trend of requiring a higher dose for the imaging of smaller features is also observed.

## CONCLUSIONS

An ArF 193nm excimer laser R&D microstepper has been developed and used to image 0.2 $\mu$ m lines and spaces in two separate photoresist materials. The overall performance of the system, including the line-narrowed excimer laser, beam diagnostics, wafer stage capabilities and the imaging lens has been characterised. Work is in progress to develop further the laser microstepper in terms of improving feature resolution by using off-axis illumination and suitable phase-shift masks at 193nm. Catadioptric imaging lenses will also be characterised and their performance compared to all-refractive designs. A fuller investigation of top-surface imaging techniques will also be undertaken to assess more fully the limits of the process at 193nm. As part of a continuing lens testing programme towards developing higher NA lenses for use at 193nm, aerial image measurements will be performed in the near future.

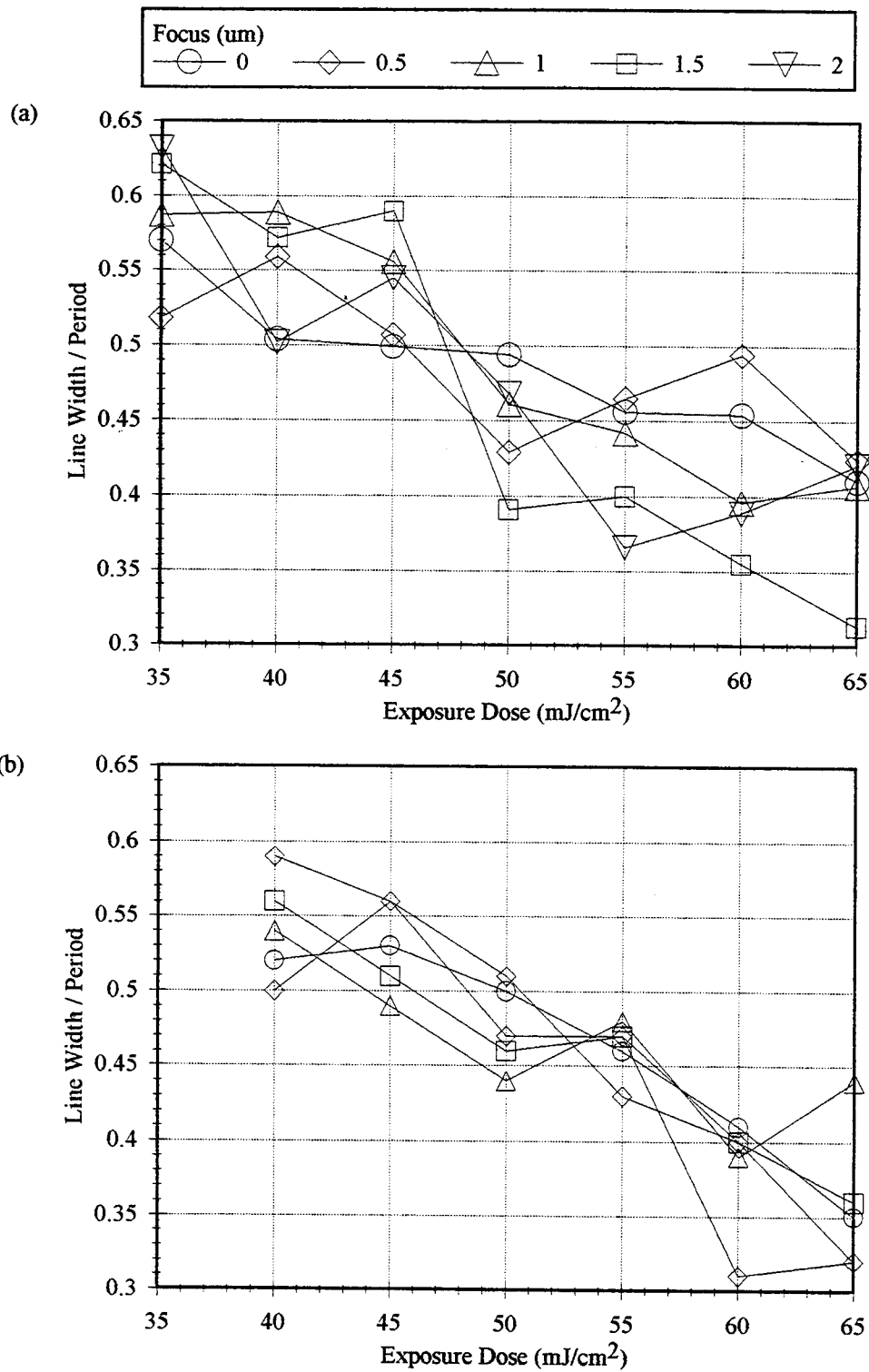


Figure 8. Exposure latitude for (a) 0.2um and (b) 0.25um lines and spaces

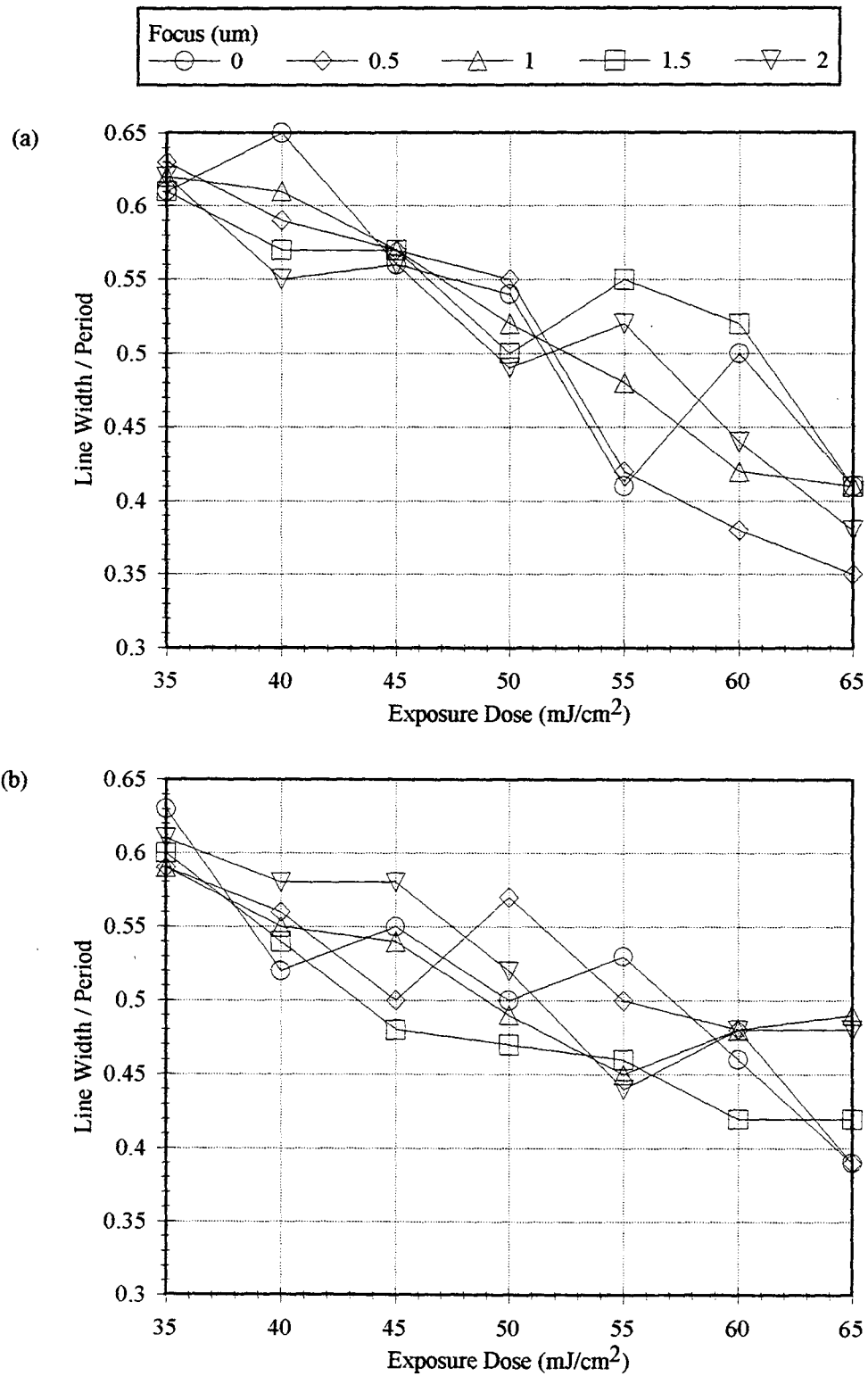


Figure 9. Exposure latitude for (a) 0.3 $\mu\text{m}$  and (b) 0.35 $\mu\text{m}$  lines and spaces

## **5. ACKNOWLEDGMENTS**

We would like to thank Graham Arthur, Geoff Thomas and Geoff Turner of the Central Microstructure Facility, RAL, for expert technical assistance.

## **6. REFERENCES**

1. M. D. Levenson, N. S. Viswanathan, R. A. Simpson, *IEEE Trans. Electron. Devices* 29, 1828 (1982)
2. M. A. Hartney, M. Rothschild, R. R. Kunz, D. J. Ehrlich, D. C. Shaver, *J. Vac. Sci. Tech. B8* (6), 1476 (1990)
3. S. C. Palmateer, A. Forte, R. Kunz, M. W. Horn, , M. Rothschild, *1st Intl. Symposium on 193nm Lithography*, Colorado Springs, Aug. 15-18 1995, Digest Session 4, Paper 9
4. B. W. Smith, A. E. Novembre, D. A. Mixon, *1st Intl. Symposium on 193nm Lithography*, Colorado Springs, Aug. 15-18 1995, Digest Session 4, Paper 11
5. D. W. Johnson, M. A. Hartney, *Jpn. J. Appl. Phys.* 31, 4321 (1992)